Available online at www.sciencedirect.com
ScienceDirect
Journal of the European Ceramic Society 31 (2011) 2205–2209
www.elsevier.com/locate/jeurceramsoc

# Creation of microcracks in porcelain during firing

František Chmelík [a,*], Anton Trník [b,c], Igor Štubňa [c], Josef Pešička [a]

[a] Department of Physics of Materials, Charles University Prague, Ke Karlovu 5, 121 16 Prague 2, Czech Republic
[b] Department of Materials Engineering and Chemistry, Czech Technical University, Thákurova 7, 166 29 Prague 6, Czech Republic
[c] Department of Physics, Constantine the Philosopher University, A. Hlinku 1, 949 74 Nitra, Slovakia

Received 24 February 2011; received in revised form 15 May 2011; accepted 25 May 2011
Available online 2 July 2011

**Abstract**

Quartz porcelain samples were tested by acoustic emission (AE) and sonic resonant methods (sensitive to nucleation and motion of structural defects) during a cooling stage of the firing process from temperature of 1250 °C. As a consequence of the mismatch of thermal expansion coefficients of the glass and the mullite phases, and the quartz particles, microcracking begun at the temperature of the glass transition (∼800 °C) and continued in several stages until the temperature reached 300 °C. A non-monotonous behaviour of the Young's modulus and temporary vanishing of the AE signals on cooling between 573 and 500 °C confirm the significance of the β → α transition, which lies mainly upon the reversal of thermal stresses acting on the glass matrix and the quartz particles. Consequently, above this temperature, radial cracks nucleating at the quartz particles appear, whereas below this temperature, circumferential cracks around the particles are produced.


*Keywords:* Porcelain; Firing; Thermal expansion; Acoustic emission; Defects; Mechanical properties

## 1. Introduction

Most of traditional ceramic materials, including quartz porcelain, have a significant amount of quartz particles in their structure. Mechanical properties of quartz porcelain are strongly influenced by its microstructure whereby unsolved quartz grains play an important role. For example, it is recognized that residual quartz grains have a negative influence on the strength of porcelain. The primary problems associated with quartz in electroporcelain and the ways to decrease the negative effects of quartz were recently described by Liebermann.[1–3] It is generally believed that the circumferential microcracks around the quartz grains observed by scanning electron microscopy (SEM) at room temperature, as shown in Fig. 1, are the result of a release of mechanical stress caused by the difference in the thermal expansion of the quartz grains and that of the glass matrix during the cooling stage of the firing. It is also assumed that these microcracks arise during the β → α transformation of the unsolved quartz grains, which is accompanied by a relatively large volume contraction ($\Delta V/V = -0.68\%$ for free quartz grain) in the temperature interval around 573 °C.[2,4–9] In spite of the importance of microcracks in quartz ceramics, the origin of the cracking has not been often studied experimentally at relevant temperatures. Experimental results were obtained by non-destructive measurements of mechanical properties linked with the crack density, e.g. of some elastic parameters, or by detection of the acoustic emission (AE) during the cooling stage of the firing. The AE technique was employed by Ohya et al.[10] to examine spontaneous cracking in porcelain samples during the cooling stage of the firing. It was observed that the AE signals appeared in the temperature range of 900–800 °C and never at temperatures lower than 600 °C. The authors assumed that their measuring system did not detect AE signals below 600 °C because of the small energy-emission rates. From the thermal expansion it was determined that the glass transformation temperature occurred at a temperature of 850 °C. Thermodilatometric data of a mullite sample and of a glass sample of the same composition as that of the glass phase in porcelain showed that the respective thermal expansions were approximately equal in the temperature range of 300–1000 °C. Consequently, thermal stresses were induced during cooling at the interfaces between the quartz grains and the glass phase. Numerous cracks frequently passing through these interfaces were observed, which indicates that either the interfaces are weak or the thermal stresses in their vicinity are

* Corresponding author. Tel.: +420 221911357; fax: +420 221911490.
*E-mail address:* chmelik@met.mff.cuni.cz (F. Chmelík).

0955-2219/$ – see front matter © 2011 Elsevier Ltd. All rights reserved.
doi:10.1016/j.jeurceramsoc.2011.05.045

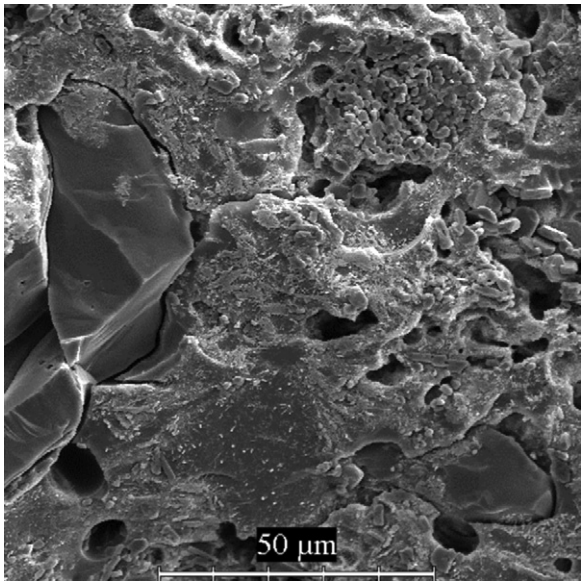


Fig. 1. Scanning electron microscopy micrograph of the fracture surface with quartz grains and circumferential cracks around them. The sample was etched with 2.5% HF for 15 s. Courtesy of the ceramic plant PPC Čab, Slovakia.

large. In our previous work,[11] a resonant measurement of the relationship between temperature and the Young's modulus (mf-TMA), which is a non-destructive method sensitive to defects in the structure (e.g. microcracks), was used for studying the mechanical behaviour of the quartz porcelain sample in the heating and cooling stages of the firing. Results obtained in[11] in the cooling stage of the firing revealed that microcracking begins at the temperature of the glass transformation $T_g$. The microcracking was expressed by slowly descending Young's modulus values below $T_g$. Then a rapid decrease of these values with a sharp minimum at ~573 °C occurred, and a small temporary increase of Young's modulus was evident during continued cooling. The cause of the recovery after $\beta \rightarrow \alpha$ quartz transformation remained unclear. A decline of the Young's modulus, and probably also creation of the microcracks were completed at the room temperature.

The object of the present work is a detailed observation and explanation of the microstructure development and microcracking in the quartz porcelain during cooling from 1000 °C to room temperature. A modulated force thermomechanical analysis (mf-TMA) and the AE technique are used to monitor the cracking and the respective microstructure development as a function of temperature. A particular attention was given to the possible origin of the small temporary increase of Young's modulus between 573 and 500 °C, mentioned in Ref. 11

## 2. Experimental

Samples were made from 50 wt.% kaolin, 25 wt.% quartz and 25 wt.% feldspar mixed with water to produce plastic ceramic material. The mineral composition of kaolin was (in wt.%): 72 kaolinite, 7 illite and montmorillonite, and 21 quartz. The mineral composition of feldspar was (in wt.%): 86 K-feldspar, 7 Na-feldspar, 2 clay and 5 quartz. The chemical composition of all substances is given in Table 1. The green cylindrical samples were made with the laboratory extruder. Dimensions of the green samples were ∅11 mm × 140 mm for mf-TMA and ∅11 mm × 60 mm for AE measurements. The green samples were fired in the air up to 1250 °C, and both analyses were performed during cooling. The temperature was increased and decreased linearly at the rate of 5 °C/min without soaking at the highest temperature.

The method used for measuring the resonant frequency was based on the flexural vibration of the sample.[12] Values of the Young's modulus $E$ at the actual temperature were calculated by using the formula:

$$E(t) = 1.26063\left(\frac{l^2 f(t)}{d}\right)^2 \rho T \quad (1)$$

where $f(t)$ is the resonant frequency of the fundamental mode at the temperature $t$; $l$, $d$ are the length and the diameter of the sample; $\rho$ is the volume mass of the material; $T = 1.02551$ is the correction coefficient for Poisson's ratio $\mu = 0.2$ and ratio $l/d = 14$, which is tabulated in Ref. 12 or calculated by the formula given in Ref. 13. Resonant frequency was measured in temperature steps of 2 °C with the apparatus described in Ref. 14.

The length and diameter also alter with the temperature, but their relative changes during cooling from 900 °C to 20 °C are less than 0.5%. The thermal contraction of the sample influences the values of Young's modulus only to a small extent and plays a non-significant role in this study.

The experimental arrangement for the AE measurement is shown in Fig. 2. The AE specimens were mounted to an end of an alumina rod, which served as a waveguide to route AE out of the furnace. A pencil break test showed a good acoustic contact between the sample and the waveguide. A miniaturised MST8S piezoelectric AE transducer (with a diameter of 3 mm, almost point AE detection, a flat response in a frequency band from 100 to 600 kHz, sensitivity of 55 dB, Ref. 1 Vef) was attached to the opposite end of the alumina rod with the help of a cyanacrylate glue. The computer controlled DAKEL-XEDO-3 AE system was used to monitor AE on the basis of two-threshold-level detection[15] (allowing a simple signal amplitude discrimination),

Table 1
The chemical composition of kaolin, feldspar and quartz used in this study. LOI – loss of ignition.

| | LOI | $SiO_2$ | $Al_2O_3$ | $Fe_2O_3$ | $TiO_2$ | CaO | MgO | $K_2O$ | $Na_2O$ | $P_2O_5$ | BaO |
|---|---|---|---|---|---|---|---|---|---|---|---|
| Kaolin | 11.50 | 55.50 | 31.26 | 0.32 | 0.16 | 0.18 | 0.23 | 0.22 | 0.22 | 0.09 | 0.32 |
| Feldspar | 0.25 | 66.30 | 17.91 | 0.04 | 0.03 | 0.03 | 0.02 | 14.60 | 0.82 | | |
| Quartz | | 99.30 | 0.38 | 0.20 | 0.02 | 0.10 | | | | | |

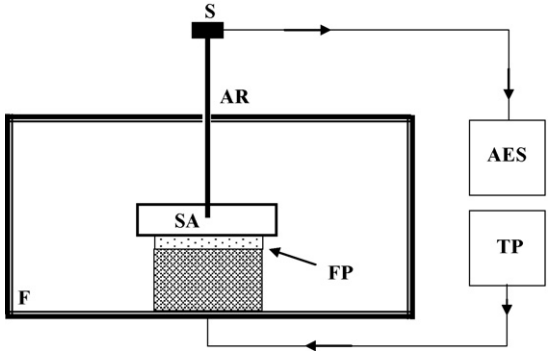


Fig. 2. Scheme of the AE measurement set up: SA – sample, AR – alumina rod (diameter 3 mm), FP – alumina fibre pad, S – AE sensor, F – furnace, TP – temperature programmer, and AES – acoustic emission system (DAKEL-XEDO box and a computer).

which yields a comprehensive set of AE parameters involving count rates (count number per second at two threshold levels, giving a total AE count and a burst AE count with proper settings—see below). The total gain was 92 dB and the AE signal sampling rate was 4 MHz. The threshold voltage for the total AE count (level 1) was set to 730 mV (slightly above the noise voltage) and the threshold voltage for the burst AE count (level 2) was 1450 mV, which allowed for the detection of large AE bursts. The full scale of the A/D converter was ±2.4 V.

## 3. Results and discussion

The mf-TMA analysis obtained during cooling is plotted in Fig. 3. A resonant flexural vibration appears in the sample if the viscosity of the glass phase is high enough for the propagation of the mechanical flexural wave. This condition occurs first at a temperature of ∼1000 °C but reliable results can be obtained below 950 °C. The magnitude of the Young modulus very slightly increases with decreasing temperature, i.e. with increasing viscosity of the glass phase, as long as the temperature of the glass transition is reached. At this point, the glass phase loses its ability to absorb the stress resulting from different thermal expansion coefficients of the two

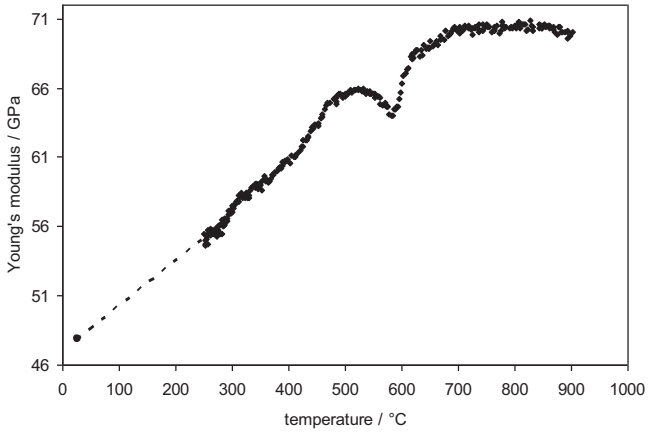


Fig. 3. Relationship between Young's modulus and temperature of green quartz sample during cooling stage of firing.

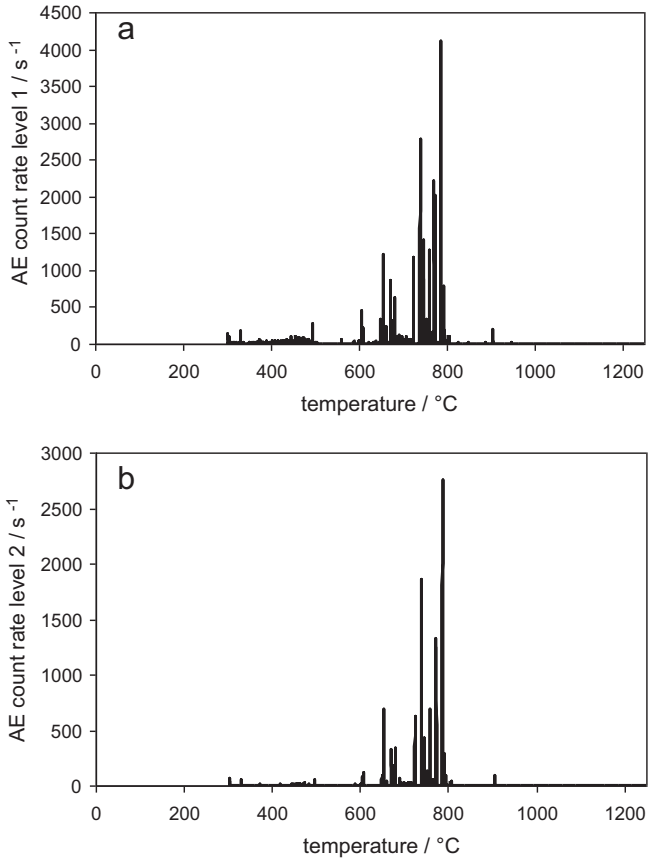


Fig. 4. (a) AE count rate from the green quartz sample during cooling. The measurement was performed with the lower AE threshold (level 1). (b) AE count rate from the green quartz sample during cooling. The measurement was performed with the higher AE threshold (level 2).

phases and microcracks can appear as a consequence of the stress relief. This process is manifested by decreasing values of the Young's modulus below ∼800 °C to a local minimum at ∼570 °C, which corresponds with the occurrence of the β → α transition. During further temperature decrease, there is a moderate and temporary recovery of the Young's modulus values, which is followed by their restored drop from 500 °C to room temperature.

Fig. 4 shows the AE count rate curves measured at both threshold levels during cooling as a function of temperature. The occurrence of intense AE signals below 800 °C correlates with the temperature of the glass transition $T_g$ and with decreasing values of the Young's modulus and reflects the formation of microcracks. The AE signals persist till the temperature of ∼600 °C and then almost disappear in the temperature interval of 600–500 °C. Consequently, most of cracks in the vicinity of the quartz grains must have been produced before the β → α transition appeared at 573 °C. On further cooling, the AE signals occur again within the temperature interval from 500 °C till 300 °C. Below 300 °C, no AE signals were observed.

In accordance with Ref. 10, the mf-TMA results and the AE analysis can be explained by taking into account the mismatch of thermal expansion coefficients of the β and α quartz phases

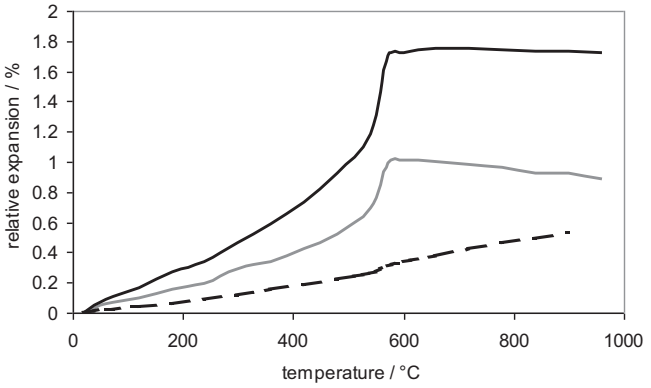


Fig. 5. Dilatometric curves of quartz single crystal for the *c*-axis (black line) and the *a*-axis (grey line),[18] and of mullite or glass in porcelain (dashed line).[19]

and the glass and mullite phases. According to Refs. 16,17, the total stress $P$ acting on the quartz particle can be calculated as

$$P = \frac{\Delta\alpha\Delta T}{(1+\mu_m)/2E_m + (1-2\mu_p)/E_p} \quad (2)$$

where $\Delta\alpha = \alpha_m - \alpha_p$ is the difference in thermal expansion coefficients of the matrix and the particles and $\Delta T$ is the magnitude of the temperature range of the cooling process. $E_m$ and $E_p$ are the Young's moduli of the matrix and the particles, respectively, and $\mu_m$ and $\mu_p$ are the Poisson's ratio values of the matrix and the particles, respectively. As experimentally found in Ref. 10, the thermal expansion coefficient of the glass phase created in porcelain and that of mullite are nearly identical. These facts represented through dilatometric curves are pictured in Fig. 5. The inspection of Fig. 5 shows further[18] that, on cooling, the quartz phase does not contract along the *c*-axis in the temperature interval from 1000 °C to 573 °C (it exhibits even dilatation along the *a*-axis in the same temperature interval). At 573 °C, there is a sharp drop of the thermal expansion, which is related to the β → α transition. The decrease of the thermal expansion slows down below 500 °C, but until the room temperature is achieved, it remains always faster than the respective thermal contraction of the glass (or mullite) phase (the thermal expansion coefficients of the glass and mullite phases are almost constant below the temperature of the glass transition).

The indicated mismatch of thermal expansion coefficients implies that, during cooling, the glass and the mullite phases will first contract more than the quartz particles and the stress according to Eq. (2) will be positive. Consequently, the matrix will stand under tensile stresses, which tend to increase with decreasing temperature, and the particles will stand under compressive stresses. Above the glass transition temperature of 800 °C these stresses are absorbed by the glass phase, but below this temperature it becomes brittle, which could result in formation of radial cracks nucleating at the quartz particles.[10,17] The nucleation and the growth of cracks are actually demonstrated by decreasing values of the Young's modulus (Fig. 3) and the occurrence of AE signals (Fig. 4). This process starts at ~800 °C and should persist until the β → α transition occurs (573 °C), as the AE signals are detected within most of this temperature interval (and not only in a part of it, as observed in Ref. 10). The β → α transition is accompanied by a fast decrease of the thermal expansion of the quartz phase. $P$ in Eq. (2) will now be negative and the quartz particles will stand under tensile stresses. Consequently, the tensile stresses acting on the matrix are rapidly relaxed and, on further cooling, the compressive stresses built up. This process of the stress reversal took place between 573 and 500 °C, demonstrating itself by vanishing of AE signals (no new cracks nucleated) and partial recovery of the Young's modulus (most likely due to healing of previously formed cracks). Below 500 °C the AE signals re-appear, which means that the newly built compressive stresses can induce an interface decohesion having character of cracks around the quartz particles. As at this stage of cooling the AE activity appeared only at the lower threshold (level 1), this process may be considered as less significant that the previous cracking under tensile stresses. Moreover, as the cooling proceeds down to room temperature, the thermal contraction of the quartz phase slows down, whereas the strength of the glass phase increases. Accordingly, the AE signals definitely disappear at temperatures below 300 °C, which indicates that no further cracking in the glass phase occurs and the ongoing decrease of the Young's modulus is rather due to accretion of already existing cracks.

## 4. Conclusions

The acoustic emission (AE) and the modulated force thermomechanical analysis (mf-TMA) technique have proven to be an efficient research tool to real time monitoring of the microstructure development and microcracking in the quartz porcelain submitted to temperature changes. Results obtained by both techniques reveal several stages of microcracking during cooling. This process begins at the temperature of the glass transition of ~800 °C and is first characterized by radial cracking nucleating at the particles (as the result of compressive stresses acting on the particle). At the temperature of the β → α transition of 573 °C, cracking is temporarily interrupted and a partial recovery of the structure occurs as the result of the thermal stresses reversal. Below 500 °C circumferential cracks around the particles appear, however, with less intensity, especially when the temperature is decreased below 300 °C.

## Acknowledgements

This work was supported by the grant VEGA 1/0216/09, Ministry of Education of Slovakia. Two of the authors (F.C., J.P.) gratefully acknowledge a financial support from the Research Goal MSM0021620834 that is financed by the Ministry of Education, Youth and Sports of the Czech Republic and from the research Grant P108/11/1267 financed by the Czech Science Foundation. The authors are indebted to the ceramic plant PPC Čab, Slovakia for supplying green ceramic samples and for the kind provision of the SEM picture obtained from investigated ceramics (Fig. 1). Helpful discussions with Prof. Z. Trojanová from Charles University Prague are also acknowledged.

## References


1. Liebermann J. About the important correlation between microstructure properties and product quality of strength-stressed high-voltage insulators. *Interceram* 2003;**53**:238–41.
2. Liebermann J. Avoiding quartz in alumina porcelain for high-voltage insulators. *Keramische Z* 2001;**53**:683–6.
3. Liebermann J. Reliability of materials for high-voltage insulators. *Am Ceram Soc Bull* 2000;**May**, www.ceramicbulletin.org.
4. Porte F, Brydson R, Rand B, Riley FL. Creep viscosity of vitreous china. *J Am Ceram Soc* 2004;**87**:923–8.
5. Carty WM, Pinto BM. Effect of filler size on the strength of porcelain bodies. *Ceram Eng Sci Proc* 2002;**23**:95–105.
6. Braganca SR, Bergman CP. Porcelain microstructure and technical properties. *Cerãmica* 2004;**50**:291–9.
7. Kozík T, Hanic F, Štubňa I. Influence of $SiO_2$ on mechanical properties of electroporcelain. III. Influence of the $\alpha \rightarrow \beta$ transformation of quartz and cristobalite on mechanical strength. *Sklář a keramik* 1988;**38**:283–5 (in Slovak).
8. Štubňa I, Kozík T, Hanic F. Influence of $SiO_2$ on mechanical properties of electroporcelain. II. Influence of the $\alpha \rightarrow \beta$ transformation of quartz and cristobalite on sound velocity. *Sklář a keramik* 1988;**38**:221–5 (in Slovak).
9. Rasch H. Interphasen-Effekte Teil. I. In porösen keramischen Gefügen. *Ceram Forum Int Ber DKG* 1995;**72**:97–102.
10. Ohya Y, Takahashi Y, Murata M, Nakagawa Z, Hamano K. Acoustic emission from a porcelain body during cooling. *J Am Ceram Soc* 1999;**82**:445–8.
11. Štubňa I, Trník A, Vozár L. Thermomechanical analysis of quartz porcelain in temperature cycles. *Ceram Int* 2007;**33**:1287–91.
12. Schreiber E, Anderson OL, Soga N. *Elastic constants and their measurement*. New York: Mc-Graw-Hill Book Co.; 1973.
13. ASTM C 1198-01, Standard test method for dynamic Young's modulus for advanced ceramics by sonic resonance. *Standard documents*. Philadelphia, USA; June 2001.
14. Štubňa I, Trník A, Vozár L. Determination of Young's modulus of ceramics from flexural vibration at elevated temperatures. *Acta Acust United Acust* 2011;**97**:1–7.
15. ASTM E 1067-85, Standard practice for acoustic emission examination of fiberglass reinforced plastic resin. *Tank/Vessels*. May 31; 1985.
16. Carty WM, Senapati U. Porcelain-raw materials, processing phase evolution, and mechanical behaviour. *J Am Ceram Soc* 1998;**81**:3–20.
17. Tenorio Cavalcante PM, Dondi M, Ercolani G, Guarini G, Melandri C, Raimondo M, et al. The influence of microstructure on the performance of white porcelain stoneware. *Ceram Int* 2004;**30**:953–63.
18. Prjanishnikov VP. *Sistema kremnezema*. Leningrad: Izd lit po stroitelstvu; 1971.
19. Pena B, Bartolomé J, Requena J, Moya JS. Mullite-alumina functionally gradient ceramics. *J Phys IV* 1993;**3**:1261–6.